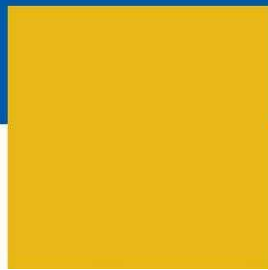
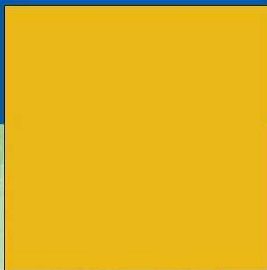




WAGENINGEN UNIVERSITY
ENVIRONMENTAL SCIENCES

AHS2005: The 2005 airborne imaging spectroscopy campaign in the Millingerwaard, the Netherlands

J.G.P.W. Clevers and L. Kooistra



CGI Report 2008-001
ISSN 1568-1874

Centre for Geo-Information (CGI)

**AHS2005: The 2005 airborne imaging spectroscopy campaign in
the Millingerwaard, the Netherlands**

J.G.P.W. Clevers and L. Kooistra

Wageningen University, Centre for Geo-Information

CGI Report 2008-01

Wageningen UR, March 2008

Contents

1	INTRODUCTION	1
2	SITE CHARACTERIZATION	2
2.1	THE FLOODPLAIN MILLINGERWAARD	2
2.2	SET-UP OF AHS CAMPAIGN	3
2.3	SET-UP OF SAMPLING PLAN FOR FIELD WORK.....	5
3	BIOPHYSICAL MEASUREMENTS	8
3.1	INTRODUCTION	8
3.2	METHODOLOGY	8
3.3	MEASUREMENT RESULTS	11
4	FIELDSPEC MEASUREMENTS	14
4.1	INTRODUCTION	14
4.2	FIELDSPEC PRO FR SPECIFICATION	14
4.3	METHODOLOGY	15
4.4	QUALITY ASSESSMENT	16
5	IMAGING SPECTROSCOPY DATA: AHS.....	19
5.1	INTRODUCTION	19
5.2	DESCRIPTION OF AHS	19
5.3	AHS MILLINGERWAARD 2005.....	20
5.4	DATA PROCESSING.....	22
6	IMAGING SPECTROSCOPY DATA: CHRIS PROBA	25
6.1	INTRODUCTION	25
6.2	DESCRIPTION OF CHRIS PROBA.....	25
6.3	ASSESSMENT OF DATA QUALITY CHRIS PROBA DATA.....	28
7	METEOROLOGICAL MEASUREMENTS.....	29
7.1	HAARWEG STATION WAGENINGEN	29
7.2	OBSERVATIONS MILLINGERWAARD.....	31
8	LAND COVER MAP MILLINGERWAARD AREA	33
9	SOIL MOISTURE AND TEMPERATURE.....	34
	REFERENCES	35
	APPENDIX 1 – AHS QUICKLOOKS MILLINGERWAARD 2005	37

1 Introduction

This report describes the field and airborne data acquired during the AHS2005 imaging spectroscopy campaign in the Millingerwaard floodplain during the summer of 2005. The acquisition of the AHS images was part of the STEREO research program (Support to the exploitation and Research in Earth Observation) of the Belgian Science Policy Office and performed in close collaboration with the Remote Sensing Laboratory of INTA, Spain, that deployed its AHS-160 hyperspectral scanner onboard of a CASA 212-200 aircraft, and VITO that organized all required operations around the flights.

The campaign is part of a research line that explores the use of hyperspectral sensors to retrieve biochemical and biophysical variables as input for ecological models using an integrated approach. The floodplain Millingerwaard was chosen to demonstrate the potential of imaging spectrometer data to support ecological modelling. The site is located along the river Rhine half way between Emmerich (D) and Nijmegen (NL) and is a typical river floodplain often found in the landscape of the Netherlands.

Several ground support teams supported the data acquisition of the AHS sensor during its flights in June 2005. Field measurements concentrated on two approaches: first, radiometric measurements were performed to support the link between soil-vegetation-atmosphere transfer modelling and secondly additional measurements were performed on vegetation to support species mapping, destructive biomass sampling, N, P and K content. Finally, also soil moisture and temperature measurements were performed.

In addition to the airborne AHS data, also spaceborne CHRIS PROBA data were collected.

In this report, the data sets derived by different instruments are discussed in separate sections in respect to their acquisition, processing and data quality.

2 Site characterization

2.1 The floodplain Millingerwaard

With the launch of the ‘Black stork’ plan (De Bruin et al., 1987) and the ideas presented in ‘Living Rivers’ (WWF, 1992), ecological rehabilitation became one of the central issues for river management in the Netherlands. Based upon these ideas, a large-scale nature rehabilitation area is developed between the cities Arnhem, Nijmegen and Emmerich called the Gelderse Poort (Figure 2.1). This crossing-border nature reserve is located along the river Rhine where it splits into three branches, viz. the Waal, the Nederrijn and the IJssel. Step by step, individual floodplains are taken out of agricultural production and are allowed to undergo their natural succession.

The floodplain Millingerwaard is part of the Gelderse Poort nature reserve (Figure 2.1). Before the 1990s, the main agricultural function of the floodplain was production grassland and arable land (e.g., maize). In the period 1990-1993, the agricultural function gradually changed into nature. Only small-scale nature management was carried out: fences between parcels were removed and cattle for natural grazing was introduced.

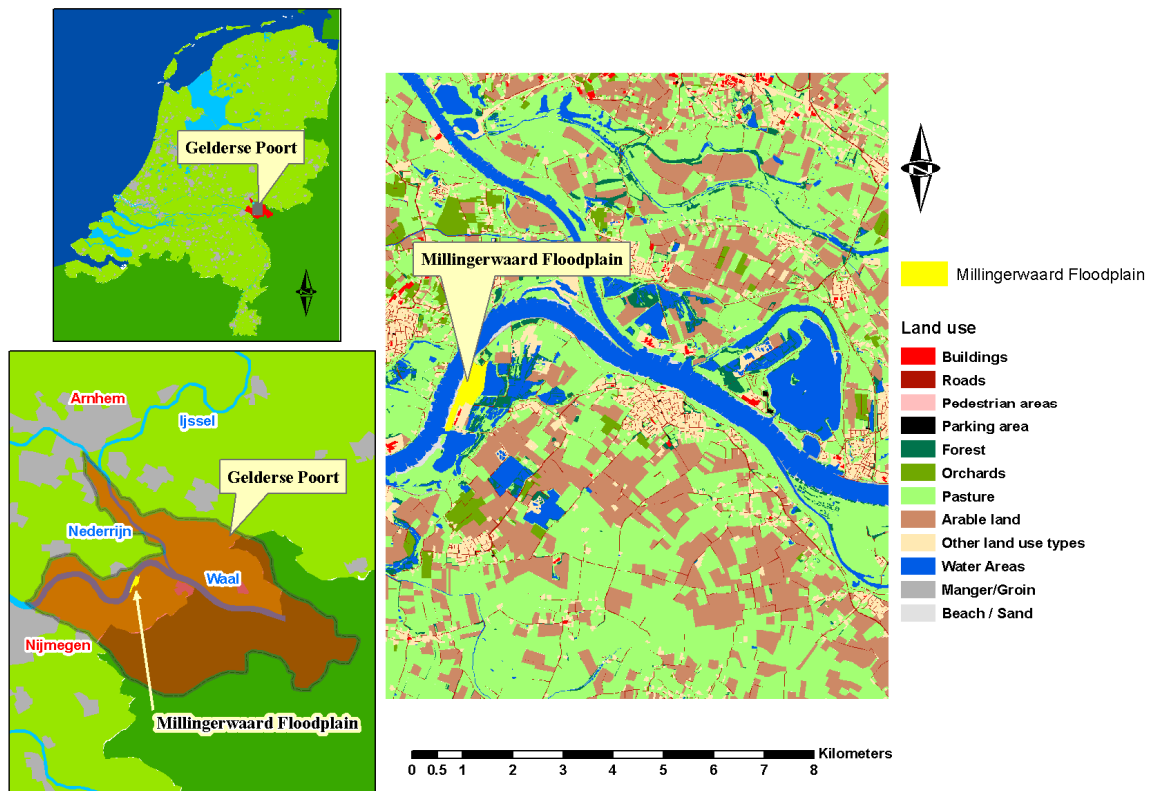


Figure 2.1: Location and current land use for the floodplain Millingerwaard along the river Rhine in the Netherlands.

To stimulate the development of a heterogeneous landscape, a low grazing density of 1 animal (e.g., Galloway, Koniks) per 2-4 ha has been chosen. This density allows grazing whole year round and also development of forest is possible. The surface area of water changes over the year. During high floods, the whole floodplain except for the higher parts of the river dunes is flooded. Due to the variability in elevation, some lower areas will be flooded for a relatively long period.

The Millingerwaard was one of the first nature rehabilitation projects for river floodplains in the Netherlands. It therefore serves as an example project for other floodplain rehabilitation projects. As a consequence a lot of effort has been put in monitoring the vegetation succession in the floodplain (Stichting Ark, Wageningen University – Nature Conservation and Plant Ecology Group). De Ronde (2003) gives an overview of the monitoring activities that have been carried out. For 1994, 1998 and 2002 reconnaissance vegetation maps are available, while a network of vegetation quadrats is monitored yearly. The monitoring focuses mainly on species composition. Information on biochemical or biophysical vegetation parameters is only limited available.

2.2 Set-up of AHS campaign

An AHS flight was scheduled for summer 2005. Four tracks were planned in different directions (figure 2.2) in order to study bidirectional reflectance characteristics of vegetation in the Millingerwaard floodplain. Finally, the flight took place on 19 June 2005 under favorable weather conditions (cf. chapter 5).

Flight Lines 2005

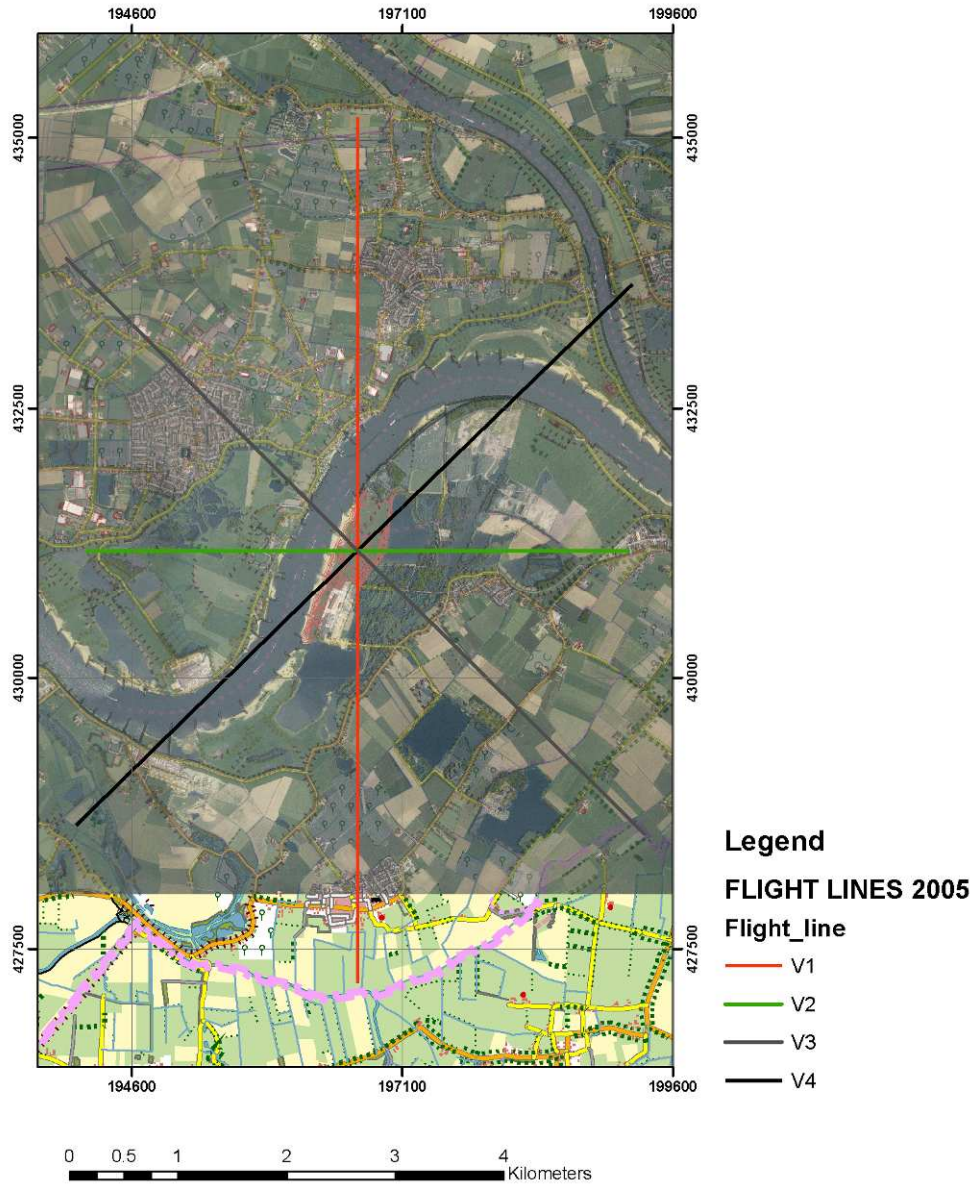


Figure 2.2: AHS flight lines in 2005 at the Millingerwaard floodplain.

2.3 Set-up of sampling plan for field work

The optimal use of the hyperspectral AHS images can only be achieved, when it is supported by a complete and accurate set of field measurements acquired during the flight. In the set-up of the sampling plan for the field work the following elements were planned:

- Measurements for radiometric correction of images;
- Measurements for radiometric characterization of vegetation;
- Destructive and non-destructive characterization of vegetation.

For radiometric correction of the AHS images, spectral measurements were made with the Fieldspec at several reference targets (e.g., bare sand, clay, asphalt, water). On the acquisition day, measurements were made for 10 locations that were distributed evenly over the flight area (Figure 2.3). Information on these locations is given in table 2.1.

Table 2.1: Location and description of the reference points used for calibrating the AHS images.

Refpoint	RD-coordinates		UTM-WGS84 (zone 31)		Cover type
	X	Y	Northing	Easting	
R25	197975	430992	5750401.30	707311.41	asphalt
R26	197534	430791	5750185.92	706877.15	asphalt
R27	197457	431300	5750692.23	706783.49	clay pit
R28	197535	432195	5751589.48	706832.14	sand
R29	197359	432410	5751798.64	706649.15	beach sand
R30	196893	431086	5750459.82	706226.70	water
R31	196973	431383	5750759.34	706296.94	water
R32	196583	431504	5750867.51	705903.11	beach sand
R33	196488	431314	5750674.47	705814.37	beach sand
R34	196413	431133	5750491.07	705745.32	beach sand

The locations for the radiometric vegetation measurements were based on the 2002 vegetation map for the Millingerwaard (Van Geloof en De Ronde, 2002) in combination with a preliminary field survey. In total 20 locations were selected, of which 6 were in the forested area. The remaining 14 sample sites were selected for vegetation sites with a range in grass, herbs and shrubs composition (Figure 2.3). Information on these locations is given in table 2.2.

Table 2.2: Location and description of the field sample locations (PFT = plant functional type).

plotnr	RD-coordinates		elevation	UTM-WGS84 (zone 31)		PFT	management
	x-coord	y-coord		Northing	Easting		
1	196764.017	430964.699	10.922	5750334.330	706101.733	grass/herbs	ungrazed
2	196430.583	430903.528	12.749	5750262.254	705770.418	grass/herbs	grazed
3	196447.569	430935.450	12.666	5750294.722	705786.352	grass/herbs	ungrazed
4	196629.206	431005.423	11.454	5750370.623	705965.634	grass/herbs	grazed
5	196595.823	431063.925	12.089	5750428.011	705930.346	grass/herbs	ungrazed
6	196530.814	431082.498	13.064	5750444.447	705864.750	grass/herbs	ungrazed
7	196637.738	431166.985	12.172	5750532.409	705968.869	shrubs	ungrazed
8	196849.471	431175.476	10.917	5750547.835	706180.251	shrubs	grazed
9	196820.848	431164.406	10.918	5750535.831	706152.001	shrubs	ungrazed
10	196862.789	431185.381	10.910	5750558.173	706193.240	shrubs	ungrazed
11	196712.081	431433.799	12.306	5750801.567	706034.443	shrubs	ungrazed
12	196622.758	431368.561	12.530	5750733.425	705947.289	grass/herbs	grazed
13	196757.438	431653.158	13.444	5751022.338	706072.596	shrubs	ungrazed
14	197086.817	432048.475	11.831	5751428.314	706388.907	grass/herbs	ungrazed
15	197376.500	431531.500		5750921.008	706695.433	forest	ungrazed
17	197382.000	431016.000		5750405.864	706717.824	forest	ungrazed
18	197242.000	430957.000		5750342.296	706579.805	forest	ungrazed
19	197255.500	430834.000		5750219.780	706597.331	forest	ungrazed
20	197015.500	430853.500		5750231.410	706356.774	forest	ungrazed

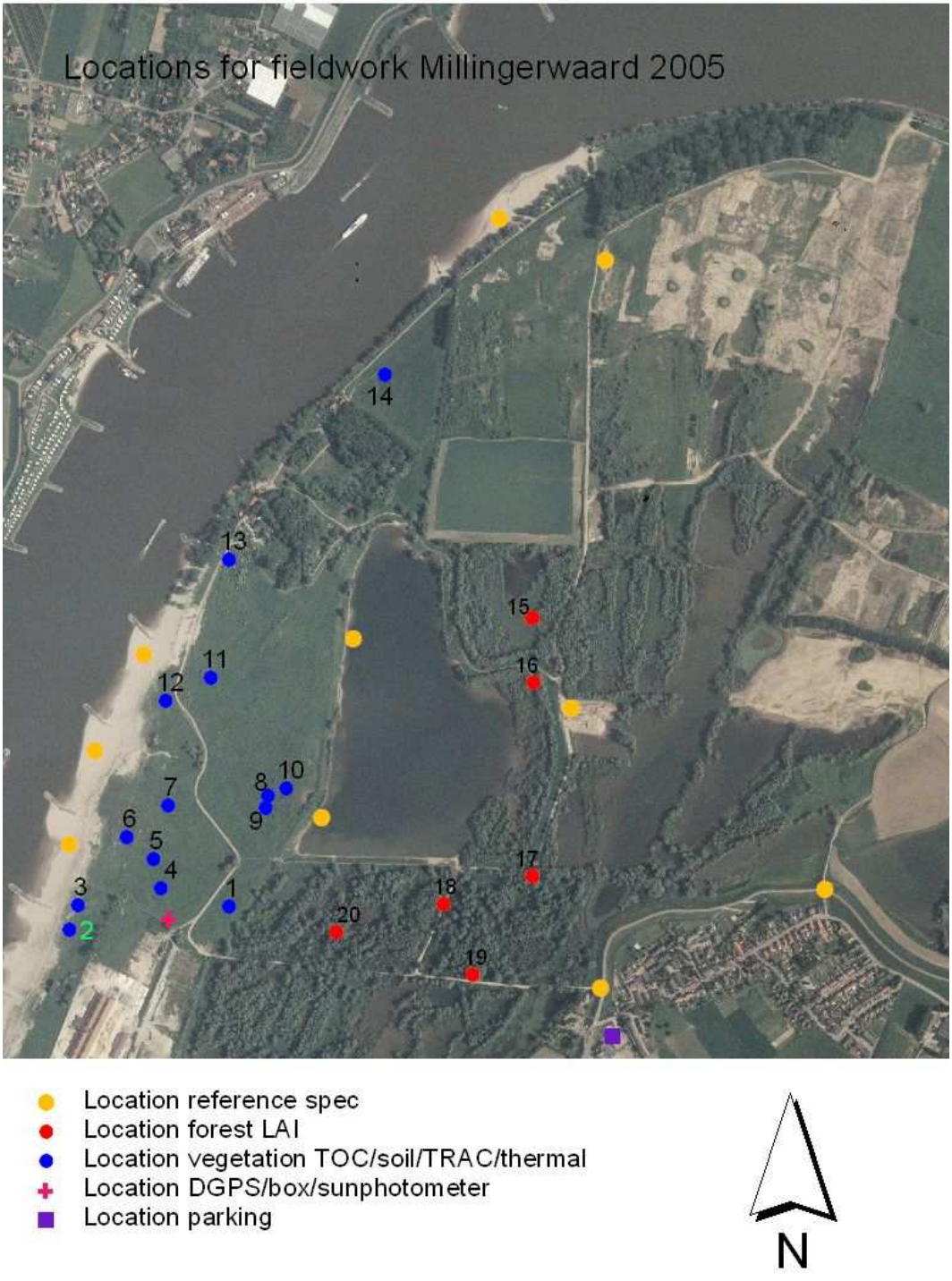


Figure 2.3: Ground based measurements for radiometric corrections and spectral characterization of vegetation within the Millingerwaard floodplain.

3 Biophysical measurements

3.1 Introduction

Main objective of the project was to explore the use of hyperspectral sensors to retrieve biophysical and biochemical vegetation parameters. During the field campaign several of these vegetation parameters were described and measured in the field and subsequently samples were analysed in the laboratory. These data are the basis for validation of the imaging spectroscopy derived products in a later stage of the project.

3.2 Methodology

Plots of 20*20 m with more or less homogeneous vegetation cover were set out according to the VALERI-protocol (figure 3.1). Every point has a letter associated to it.

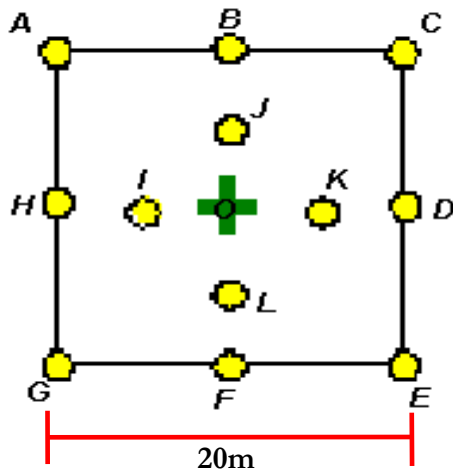


Figure 3.1: Experimental set-up of sampling plot according to VALERI-protocol (www.avignon.inra.fr/valeri/).

A description of the vegetation was made for the 14 vegetation plots (20 x 20 m) that were also radiometrically characterized. Locations of the plots are shown in Figure 2.3.

Vegetation description

Vegetation descriptions were made according to the method of Braun-Blanquet (1951). Abundance per species was estimated optically as percentage soil covered by living biomass in vertical projection, and scored in a nine-point scale. All bryophytes and lichens, and also vascular species that were not readily recognisable in the field,

were collected for later identification. *Taraxacum* species were taken together as *T. vulgare*, and *Rubus* species were taken together as *R. fruticosus*, except *R. caesius*. No subspecific taxa were used. Nomenclature follows van der Meijden et al. (1990), Touw & Rubers (1989), and Brand et al. (1988) for vascular species, mosses and lichens, respectively. No distinction in layers (e.g. by using pseudo-species) was made. Syntaxonomic nomenclature follows Schaminée et al. (1995, 1996, 1998).

Biomass

Vegetation biomass was sampled in three subplots with a relatively homogeneous (vegetation) cover measuring 0.5 x 0.5 m, located within the Valeri-plots. Biomass was clipped at 0.5 cm above the ground level and stored in paper bags. The collected material was weighted for fresh biomass, then it was dried for 24 h at 70°C, and weighed again.

LAI estimation

Three instruments were used for determining leaf area index (LAI) of sample areas. These are the LAI-2000 and TRAC instruments and the use of hemispherical photography.

LAI-2000. The LAI-2000 (figure 3.2) uses a fish-eye lens with a hemispheric field of view ($\pm 148^\circ$). The detector is composed of five concentric rings (sensitive to radiation below 490 nm). Each ring responds over a different range of zenith angles. The radiation is therefore azimuthally integrated. The LAI-2000 instrument measures the fraction of diffuse incident radiation that passes through a plant canopy for a given view zenith angle, assuming that the foliage is azimuthally randomly oriented. Then the ratio is calculated between a below-canopy and an above-canopy measurement. As LAI-2000 is based on the transmittance measurement, it is important to notice that it allows to derive an effective plant area index rather than the leaf area index which is defined as the total one-sided leaf area of photosynthetic tissue per unit horizontal ground surface area. Indeed, all canopy elements that appear black under 490 nm (trunks, flowers, yellow grass,...) are taken into account in the computation of LAI.



Figure 3.2: LAI-2000 instrument.

TRAC. TRAC (figure 3.3) is an optical instrument for measuring the leaf area index (LAI) and the fraction of photosynthetically active radiation absorbed by plant canopies (FPAR). TRAC measures canopy 'gap size' distribution in addition to canopy 'gap fraction'. Gap fraction is the percentage of gaps in the canopy at a given solar zenith angle. It is usually obtained from radiation transmittance. Gap size is the physical dimension of a gap in the canopy. For the same gap fraction, gap size distributions can be quite different. TRAC (including the recording and data analysis components) is hand-carried by a person walking at a steady pace (about 0.3 meter per second). Using the solar beam as a probe, TRAC records the transmitted direct light at a high frequency. The clumping index obtained from TRAC can be used to convert effective LAI to LAI. When TRAC is used for half a clear day, an accurate LAI value can also be obtained using TRAC alone.



Figure 3.3: TRAC instrument.

Hemispherical photography. The use of hemispherical cameras (figure 3.4) is interesting when attempting to improve the estimation of the gap fraction, since hemispherical photography is a convenient technique that offers the potential to account for foliage clumpiness and greenness confusion that may significantly affect the characterization of important vegetation types (Fernandes et al., 2002; Weiss et al., 2004; Jonckheere et al., 2004). Dedicated neural network system software (CAN_EYE) was used to process these colour photographs. This software places its emphasis on green element classification and processing of series of photographs. LAI and gap fraction of the forests was calculated using the same software. Algorithms developed for LAI calculations derived from hemispherical sensors involve a division of 2π steradian (180°) field of view (FOV) into concentric equi-angular annuli. From image processing systems like hemispherical photos, the gap fraction for each of these annuli is the ratio between the number of pixels in a gap (pixel illuminated by the sky) and the total number of pixels in this angular sector. Finally, gap fraction measurements were used to estimate the LAI of canopies with an assumption of a random distribution of vegetation elements (canopy elements).



Figure 3.4: Example of a hemispherical photograph.

Biochemistry

Sampled vegetation material for the vegetation plots was chemically analyzed for N, P, K, Ca and Mg content (mmol/kg).

Table 3.1: Classified vegetation syntax for the individual plots in the Millingerwaard.

plotid	Associa_01	Associa_02	Associa_03	SYNTAXON	NEDNAAM
1	33RG01	32RG06	31RG05	RG <i>Urtica dioica</i> -[Galio-Urticetea]	Rompgemeenschap van Grote brandnetel
2	31CA02	31CA03B	14BC02B	Echio-Melilotetum	Honingklaver-associatie
3	31CA02	16BB01B	16BB01D	Echio-Melilotetum	Honingklaver-associatie
4	33AA05B	38AA01B	31CA03B	Urtico-Aegopodietum holcetosum	Zevenblad-ass.; subass. met Gestreepte witbol
5	31CA03B	31CA02	33AA04B	Tanaceto-Artemisietum typicum	Wormkruid-ass.; typische subass.
6	31CA02	14BC02B	16BB01D	Echio-Melilotetum	Honingklaver-associatie
7	31CA02	31CA03B	33AA03A	Echio-Melilotetum	Honingklaver-associatie
8	38AA01B	31CA02	31CA01B	Artemisio-Salicetum agrostietosum stoloniferae	Bijvoet-ooibos; subass. met Fioringras
9	38AA01B	31CA01B	31CA03B	Artemisio-Salicetum agrostietosum stoloniferae	Bijvoet-ooibos; subass. met Fioringras
10	37AB01A	33DG02	43RG02	Pruno-Crataegetum	Associatie van Sleedoorn en Eenstijlige meidoorn
11	33RG03	38AA01B	31CA03B	RG <i>Petasites hybridus</i> -[Galio-Urticetea]	Rompgemeenschap van Groot hoefblad
12	31CA02	14BC02B	31CA01B	Echio-Melilotetum	
13	43RG02	37AB01A	38RG01	RG <i>Urtica dioica</i> -[Ulmenion carpinifoliae]	Rompgemeenschap van Grote brandnetel
14	16BC01A	31CA01B	12RG01	Lolio-Cynosuretum typicum	Kamgrasweide; typische subass.
15					
16					
17	38AA03C	37AB01A	38RG01	Cardamino amarae-Salicetum urticetosum	Bittere veldkers-ooibos; subass. met Grote brandnetel
18	38RG01	38AA03C	32RG06	RG <i>Urtica dioica</i> -[Salicion albae]	Rompgemeenschap van Grote brandnetel
19	38RG01	38AA03C	37AB01A	RG <i>Urtica dioica</i> -[Salicion albae]	Rompgemeenschap van Grote brandnetel
20	38RG01	32RG06	33RG01	RG <i>Urtica dioica</i> -[Salicion albae]	Rompgemeenschap van Grote brandnetel

3.3 Measurement results

In total, 79 species were found in the vegetation plots in the Millingerwaard. The plots were syntaxonomically identified by the program ASSOCIA (table 3.1). Values for the measured fresh and dry weight and results of the biochemical analysis per

sample are presented in table 3.2 and average values per plot are presented in table 3.3. Plot 11 and 13 were not harvested due to the presence of large shrubs of *Sambucus nigra*.

Table 3.2: Measured weight and biochemical variables for the individual samples in the Millingerwaard in 2005. For plot 6 and 7 no biochemicals of subplots were obtained and for plot 8 no biochemicals at all were obtained.

	Plot	VALERI	fresh weight	dry weight	N	P	K
PFT	Nr.	location	g/m ²	g/m ²	mmol/kg		
shrub	1	A	4737.56	923.84	1278	78	737
shrub	1	C	3525.2	433.08	1248	109	897
shrub	1	E	4999.48	1027.24	1035	87	600
herb	2	A	555.68	113.6	1049	65	676
herb	2	C	1613.88	380.24	925	88	571
herb	2	E	2106	528.12	901	86	604
herb	3	A	497.88	101.6	773	107	468
herb	3	C	679	194.84	987	114	582
herb	3	E	1561.4	296.44	1224	123	690
herb	4	A	2114.48	456.6	1016	102	795
herb	4	C	957.92	196.88	1305	98	646
herb	4	E	2538.88	562.84	1306	94	784
shrub	5	A	2050.56	540.88	1136	99	589
shrub	5	C	2312.92	684.16	1079	82	429
shrub	5	E	3661.72	1170.96	965	82	535
herb	6	A	881.76	141	943	87	590
herb	6	C	635.12	133.56	-	-	-
herb	6	E	682.16	143	-	-	-
herb	7	A	2687.2	680.4	1176	83	570
herb	7	C	1767.12	589.84	-	-	-
herb	7	E	1866.28	357.84	-	-	-
herb	8	A	1518.84	487.36	-	-	-
herb	8	C	1331.72	286.48	-	-	-
herb	8	E	1105.84	242.4	-	-	-
shrub	9	A	4570.12	1155.44	916	85	621
shrub	9	C	4107.4	1115.72	1024	89	539
shrub	9	E	1247.4	333.48	1017	88	460
shrub	10	A	2747.88	485.32	986	111	720
shrub	10	C	1998.04	641.8	1089	75	371
shrub	10	E	2967.2	597.4	1335	119	757
herb	12	A	429.12	84.04	1050	99	532
herb	12	C	271	31.6	1289	88	467
herb	12	E	489.84	115.64	1026	99	505
herb	14	A	803.08	151.04	1421	128	831
herb	14	C	1505.12	314.24	847	99	668

Table 3.3: Measured weight and biochemical variables for the individual plots in the Millingerwaard in 2005.

Plot	fresh weight	dry weight	water weight	N	P	K
Nr.	g/m ²	g/m ²	g/m ²	mmol/kg		
1	4420.75	794.72	3626.03	1187.0	91.4	744.5
2	1425.19	340.65	1084.53	958.5	79.7	616.8
3	912.76	197.63	715.13	994.3	114.6	580.0
4	1870.43	405.44	1464.99	1208.8	97.8	741.4
5	2675.07	798.67	1876.40	1059.8	87.5	517.7
6	733.01	139.19	593.83	942.9	87.4	590.3
7	2106.87	542.69	1564.17	1175.9	82.6	570.4
8	1318.80	338.75	980.05	-	-	-
9	3308.31	868.21	2440.09	985.6	87.4	540.0
10	2571.04	574.84	1996.20	1136.8	101.8	616.1
11				-	-	-
12	396.65	77.09	319.56	1121.9	95.2	501.3
13				-	-	-
14	1154.10	232.64	921.46	1134.0	113.5	749.4

Table 3.4: Results of LAI estimates using different techniques for the individual plots in the Millingerwaard in 2005. More details can be found in Gonsamo, 2006.

Plot Nr.	PFT	LAI-2000		TRAC	Hemispherical photo	
		2 rings	5 rings		HP LAI	HP30 LAI
1	GH	4.93	3.91	2.44	10	5.8
2	GH	2.46	2.01	1.2	5.9	8.9
3	GH	1.69	1.42	0.7	5.1	6.9
4	GH	7.51	5.28	2.85	3.8	5.7
5	GH			4.28	5.6	4.3
6	GH	3.35		1.41	6.8	10
7	SH	10.99			6.5	10
8	SH	6.47	4.34	1.82	3.71	4.62
9	SH	10.46			4.12	9.86
10	SH				6.66	
11	SH	9.5	5.87	1.48	6.16	11.6
12	GH	4.9	3.2		6.9	9.6
13	SH	8.89	5.02	5.58	8.82	12.15
14	GH	3.31			5.3	6.3
15	FR			5.25	5.75	
17	FR				10.58	
18	FR				10.49	
19	FR			5.59	10.14	
20	FR			5.91		

4 FieldSpec measurements

4.1 Introduction

June 19th, 2005, a field campaign with an ASD FieldSpec Pro FR spectroradiometer was performed at the Millingerwaard site. For every plot 12 measurements were performed according to the VALERI sampling scheme, whereby each measurement was the average of 15 readings at the same spot. Measurement height was about 1 m above the vegetation. A Spectralon white reference panel was used for calibration.

The FieldSpec instrument is built by Analytical Spectral Devices (ASD) in the US. It has the following advanced features (ASD, 2005):

- A notebook-sized, Windows based computer interface providing functional access to all instrument controls and real-time display of spectral data;
- A flexible 1.5 m fiber optic cable with a 25° field of view that allows rapid scanning and data collection over large target areas;
- RS3 advanced remote sensing software for trouble-free data acquisition and storage;
- DriftLock™ dark current compensation to ensure high accuracy;
- Compact housing in an ergonomic and adjustable field backpack;
- A powerful NiMH battery providing 4 hours of portable operation.

4.2 FieldSpec Pro FR specification

Table 4.1: Specifications of the FieldSpec PRO FR spectroradiometer (ASD, 2005).

Spectral range	350 - 2500 nm
Spectral resolution	3 nm @ 700 nm 10 nm @ 1400/ 2100 nm
Sampling interval	1.4 nm @ 350 - 1050 nm 2 nm @ 1000 - 2500 nm
Scanning time	100 milliseconds
Detectors	One 512 element Si photodiode array 350 - 1000 nm Two separate, TE cooled, graded index InGaAs photodiodes 1000 - 2500 nm
Input	Optional foreoptics available
Noise Equivalent Radiance (NeDL)	UV/VNIR 1.4×10^{-9} W/cm ² /nm/sr @ 700nm NIR 2.4×10^{-9} W/cm ² /nm/sr @ 1400nm NIR 8.8×10^{-9} W/cm ² /nm/sr @ 2100nm
Weight	7.2 kg
Notebook Computer	1 GHz processor, 256 MB Ram, 20GB Hard Disk Drive, 1024x768 graphics resolution, 24 bit color, bi-directional parallel port, AC/DC adapter/charger, 64 MB USB Flash memory drive

4.3 Methodology

The spectral measurements were conducted parallel to the AHS overflights to meet identical illumination conditions. Measurement locations were georeferenced by handheld GPS and DGPS measurements. Locations for spectral characterisation of the vegetation canopy were determined in advance. Based on the available vegetation map for the Millingerwaard (2002) and a survey in the area, 14 locations with specific vegetation structure types were selected (Figure 2.3). Figure 4.2 gives an overview of the measurements performed on 19 June 2005 over the vegetation plots.

In addition, 10 locations were selected that are spectrally flat and temporally stable (see table 2.1). These can be used for calibrating the airborne images. Figure 4.2 gives an overview of the measurements performed on 19 June 2005 over the calibration sites.

Data processing spectra

The collected spectra were first exported to ASCII files with the FieldSpec Pro software. One ASCII file was created for each separate spectrum. Subsequently, all the data were imported into Microsoft Excel for further processing. For each object, mean and standard deviation of the available spectra were calculated.

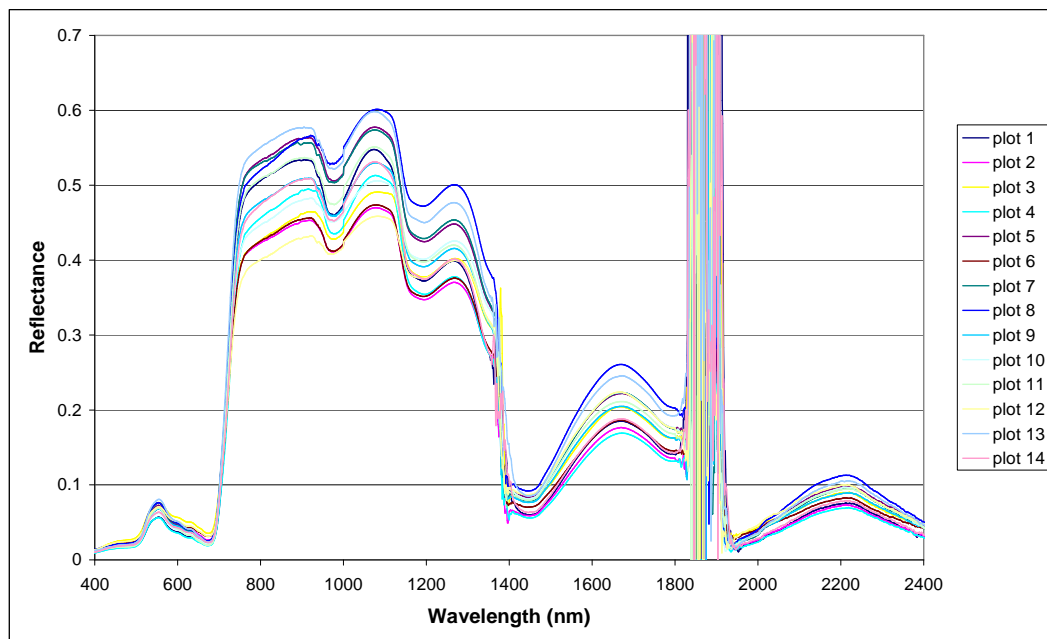


Figure 4.1: Example of 14 FieldSpec measurements on the vegetation plots at the Millingerwaard site in 2005.

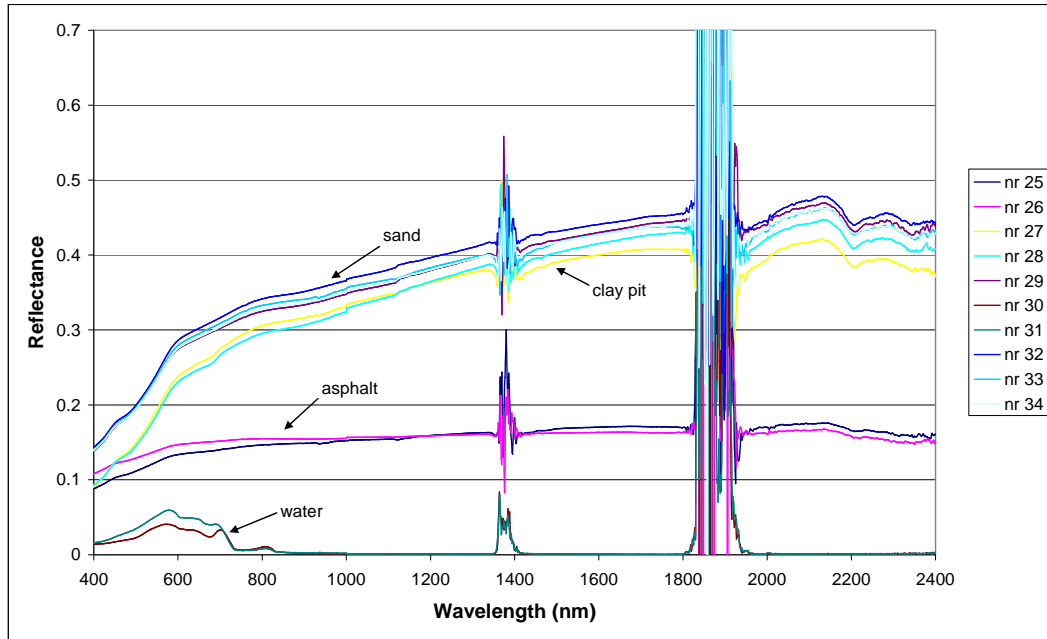


Figure 4.2: Example of 10 FieldSpec measurements on the calibration plots at the Millingerwaard site in 2005.

4.4 Quality assessment

As a first step, all spectra were visually analysed in order to detect clearly wrong spectra. No spectra were removed at this step.

Subsequently, the measurements of the Spectralon reference at the end of each object measurement were checked. Ideally, this spectrum should be yielding a reflectance of 1.0 all over the spectrum in all cases. Although small deviations were observed, it was concluded that deviations in all cases were that small that no further calibration was needed. Figure 4.3 shows an example of such a Spectralon measurement.

Step 3 was the removal of noisy parts of the spectrum from all spectra. Spectra for the wavelengths 2401 – 2500 nm were removed due to the high instrument noise observed in the spectra. Water absorption bands ranging from 1350 – 1450 nm and from 1800- 1950 nm were removed from the dataset too. Figure 4.4 shows the final result.

Finally, a picture was taken of every object measured with the FieldSpec spectroradiometer. Figure 4.5 shows an example.

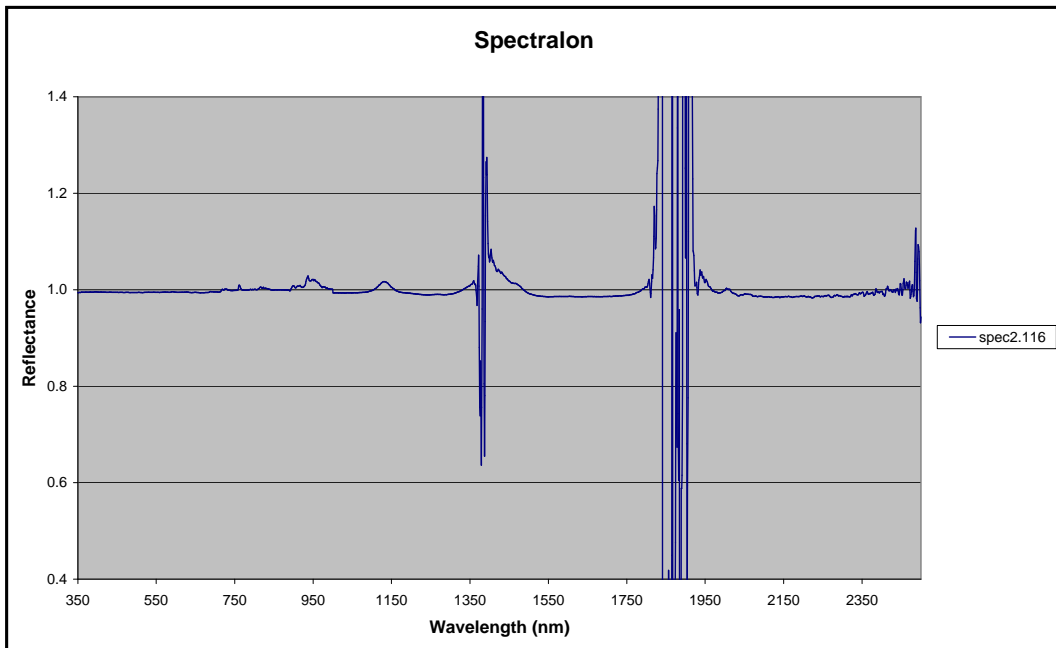


Figure 4.3: FieldSpec measurement of the Spectralon calibration panel.

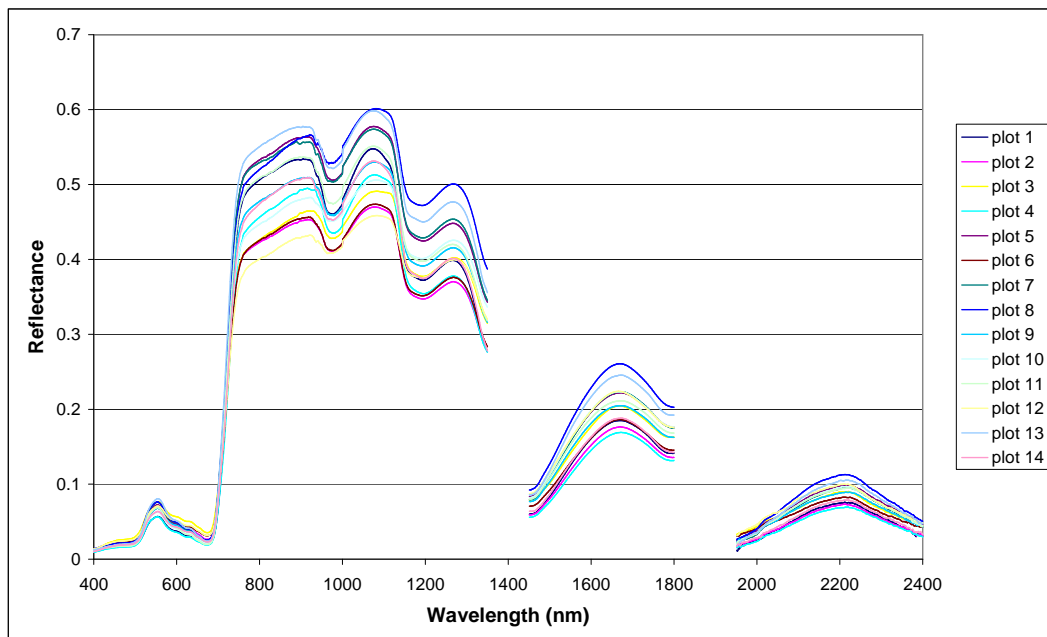


Figure 4.4: The example from figure 4.1 after removing the noisy measurements.



Figure 4.5: Digital photograph of the vegetation area at the Millingerwaard site.

5 Imaging spectroscopy data: AHS

5.1 Introduction

On 19 June 2005 a flight with the AHS sensor was performed by the Remote Sensing Laboratory of the Instituto Nacional de Técnica Aeroespacial (INTA) in Spain.

5.2 Description of AHS

The AHS sensor (Airborne Hyperspectral Scanner) is an airborne imaging 80-band line scanner radiometer based on the whiskbroom technique. It can be considered a powerful tool for applications in which high spectral, radiometric and spatial detail is required while keeping a wide spectral coverage.



Figure 5.1: The AHS system.

The instrument has been installed in the INTA's aircraft (CASA C-212), and is integrated with a GPS/INS POS-AV 410 from Applanix.

Some specifications:

- Optical design: scan mirror plus reflective optics with a single IFOV determining field stop
- FOV (Field of View): 90°
- IFOV (Instantaneous Field of View): 2.5 mrad
- GSD (Ground Sampling Distance): 2.1 mrad (0.12 degrees)
- Scan rates: 12.5, 18.75, 25, 35 r.p.s., with corresponding ground sampling distances from 7 to 2 meters
- Digitization precision: 12 bits to sample the analog signal, with gain level from $\times 0.25$ to $\times 10$
- Samples per scan line: 750 pixels/line
- Reference sources: two controllable thermal black bodies within the field of view, set to a temperature range from -15°C to $+25^{\circ}\text{C}$ with respect to scan head heat sink temperature
- Spectrometer: four dichroic filters to split radiation in four optical ports, and diffraction gratings within each port
- Detectors: Si array for VIS/NIR port; InSb and MCT arrays, cooled in N_2 dewars, for SWIR, MIR and TIR ports.

Table 5.1: Specifications of the four optical ports of the AHS sensor.

	Port 1	Port 2A	Port 2	Port 3	Port 4
Interval (μm)	0.43 – 1.03	1.55 – 1.65	1.9 – 2.55	3.3 – 5.4	8.2 – 12.7
FWHM (nm)	30	90	18	300	450
#bands	20	1	42	7	10

Table 5.2: AHS pixel size versus flight parameters.

Scan rate (rps)	Ground speed (Kts)	Flying height (m)	GIFOV (m)	Swath (m)
6.25	140	5491	13.73	10982
12.5	140	2745	6.86	5491
18.7	140	1835	4.59	3670
25	140	1373	3.43	2745
31.2	140	1100	2.75	2200
35	140	981	2.45	1961

5.3 AHS Millingerwaard 2005

The quick looks of the 4 flight lines recorded over the Millingerwaard area on 19 June 2005 are shown in Appendix 1. 63 Bands in the reflective part of the EM spectrum have been recorded. Specifications of the spectral bands are given in table 5.3.

Table 5.3: Characteristics of the spectral bands (in μm) as derived from the header data of the AHS images for the Millingerwaard in 2005.

Band	Begin	End	Centre	Width	FWHM
1	0.4206	0.4894	0.455	0.0688	0.027
2	0.4483	0.5197	0.484	0.0714	0.028
3	0.4761	0.5499	0.513	0.0738	0.029
4	0.5063	0.5777	0.542	0.0714	0.028
5	0.5353	0.6067	0.571	0.0714	0.028
6	0.5653	0.6367	0.601	0.0714	0.028
7	0.5943	0.6657	0.630	0.0714	0.028
8	0.6233	0.6947	0.659	0.0714	0.028
9	0.6533	0.7247	0.689	0.0714	0.028
10	0.6823	0.7537	0.718	0.0714	0.028
11	0.7116	0.7804	0.746	0.0688	0.027
12	0.7396	0.8084	0.774	0.0688	0.027
13	0.7683	0.8397	0.804	0.0714	0.028
14	0.7973	0.8687	0.833	0.0714	0.028
15	0.8263	0.8977	0.862	0.0714	0.028
16	0.8566	0.9254	0.891	0.0688	0.027
17	0.8823	0.9537	0.918	0.0714	0.028
18	0.9123	0.9837	0.948	0.0714	0.028
19	0.9393	1.0107	0.975	0.0714	0.028
20	0.9658	1.0422	1.004	0.0764	0.030
21	1.4194	1.8246	1.622	0.4052	0.159
22	2.0141	2.0479	2.031	0.0338	0.013
23	2.0260	2.0598	2.043	0.0338	0.013
24	2.0387	2.0723	2.056	0.0336	0.013
25	2.0512	2.0848	2.068	0.0336	0.013
26	2.0631	2.0967	2.080	0.0336	0.013
27	2.0757	2.1091	2.092	0.0334	0.013
28	2.0873	2.1205	2.104	0.0332	0.013
29	2.0998	2.1330	2.116	0.0332	0.013
30	2.1119	2.1447	2.128	0.0328	0.013
31	2.1233	2.1565	2.140	0.0332	0.013
32	2.1351	2.1683	2.152	0.0332	0.013
33	2.1467	2.1801	2.163	0.0334	0.013
34	2.1585	2.1921	2.175	0.0336	0.013
35	2.1693	2.2025	2.186	0.0332	0.013
36	2.1818	2.2152	2.199	0.0334	0.013
37	2.1933	2.2265	2.210	0.0332	0.013
38	2.2046	2.2378	2.221	0.0332	0.013
39	2.2159	2.2491	2.233	0.0332	0.013
40	2.2275	2.2607	2.244	0.0332	0.013
41	2.2388	2.2722	2.256	0.0334	0.013

42	2.2497	2.2829	2.266	0.0332	0.013
43	2.2666	2.3002	2.283	0.0336	0.013
44	2.2778	2.3112	2.295	0.0334	0.013
45	2.2891	2.3223	2.306	0.0332	0.013
46	2.2993	2.3329	2.316	0.0336	0.013
47	2.3100	2.3434	2.327	0.0334	0.013
48	2.3203	2.3537	2.337	0.0334	0.013
49	2.3314	2.3648	2.348	0.0334	0.013
50	2.3424	2.3758	2.359	0.0334	0.013
51	2.3530	2.3862	2.370	0.0332	0.013
52	2.3640	2.3968	2.380	0.0328	0.013
53	2.3744	2.4070	2.391	0.0326	0.013
54	2.3844	2.4172	2.401	0.0328	0.013
55	2.3945	2.4273	2.411	0.0328	0.013
56	2.4046	2.4374	2.421	0.0328	0.013
57	2.4157	2.4489	2.432	0.0332	0.013
58	2.4261	2.4575	2.442	0.0314	0.012
59	2.4361	2.4687	2.452	0.0326	0.013
60	2.4459	2.4783	2.462	0.0324	0.013
61	2.4555	2.4879	2.472	0.0324	0.013
62	2.4667	2.4983	2.483	0.0316	0.012
63	2.4757	2.5075	2.492	0.0318	0.013

5.4 Data processing

The flight lines over the Millingerwaard were performed at an altitude of 1900 m (a.s.l.), resulting in a pixel size of 4.73 m (IFOV is 2.5 mrad). The images were geometrically coregistered with orthophotos obtained in 2004 at a spatial resolution of 1 m and using the Dutch National Coordinate system (RD) as a reference using the PARGE software (Schläpfer & Richter, 2002) at VITO (Flemish Institute for Technological Research). The final pixel size was 5 m. AHS data were delivered in the map projection UTM (Zone 31, geodetic datum WGS84).

Radiometric preprocessing and atmospheric correction of the image was performed at VITO using a MODTRAN4 (Berk et al., 1999) and ATCOR4 (Richter & Schläpfer, 2002) radiative transfer code and by using FieldSpec measurements performed in the field on reference targets (water, beach sand and asphalt) for iteratively improving the parameters describing the atmospheric composition (i.e. visibility, water vapour and aerosol type) for the whole image. This resulted into calibrated surface reflectance values (with an offset value of 10 and a gain value of 65525).

However, checking the surface reflectances derived from the AHS image showed that the calibration was not that good. Therefore, an additional empirical line correction procedure was applied using the same reference targets. Finally, spectral

signatures were derived using the GPS coordinates of the field plots by averaging over a 3 by 3 window (since the field plots were 20 by 20 m).

In 2007 VITO performed a reprocessing of the 2005 images using an atmospheric correction procedure based on the estimation of atmospheric water vapour per pixel instead of doing this for an image as a whole. This is based on a paper by Rodger & Lynch (2001). Improved correction for visibility is based on a paper by Richter et al. (2006). More information on the total pre-processing workflow at VITO can be found in Biesemans et al. (2007).

Figure 5.2 shows an example of some spectral signatures derived from the re-processed images.

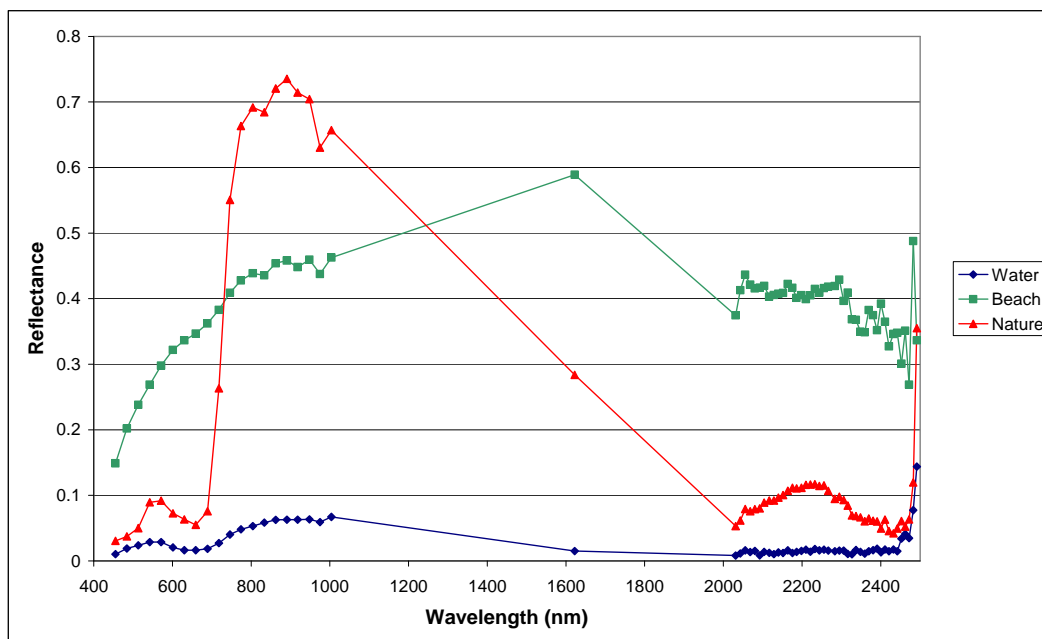


Figure 5.2: Three spectral signatures as derived from the AHS images for the Millingerwaard test area in 2005.

Images are delivered by VITO in HDF5 format. HDF stand for Hierarchical Data Format and it is a library and multi-object file format often used for the transfer of graphical and numerical data between computers. Conversion to Envi files is performed by using the software tool GeoExtract delivered by VITO together with the images.

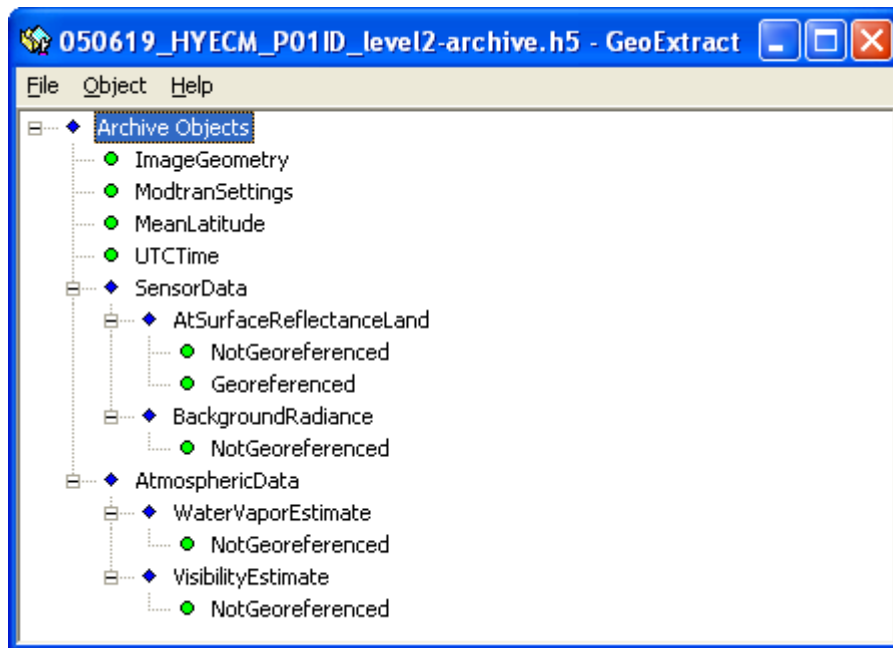


Figure 5.3: GeoExtract window showing the information present in the AHS files.

Figure 5.3 shows that the data contain information on image geometry, Modtran settings, latitude information per scanline, UCT time per scanline (not georeferenced). The data are delivered as both georeferenced and not georeferenced images in 63 spectral bands. Due to the georeferencing the size of the georeferenced image may increase dramatically. In addition a background radiance level is given (not georeferenced). Finally, estimates of water vapour and visibility are provided per pixel (both not georeferenced). The image geometry is also given for the not georeferenced images and consists of values for each pixel for:

- X coordinate
- Y coordinate
- Elevation
- Solar zenith angle (degrees)
- Relative azimuth angle (degrees)
- View zenith angle (degrees)
- Solar azimuth angle in degrees (N = 0, E = 90, etc.)
- View azimuth angle in degrees (N = 0, E = 90, etc.)
- Euclidean distance between observation point and target point in meter.

6 Imaging spectroscopy data: CHRIS PROBA

6.1 Introduction

During the 2005 campaign also CHRIS PROBA data were acquired for the area around Millingerwaard on September 6, 2005. The data quality description in this chapter is aiming at a full assessment of potential shortcomings present in the CHRIS PROBA data. At the end of the chapter there will be recommendations for the further use of the data.

6.2 Description of CHRIS PROBA

CHRIS (Compact High Resolution Imaging Spectrometer) is a physically compact payload as its name implies (weighing under 15 kg) and operates in the 'push-broom' mode¹. The telescope in the CHRIS instrument is nadir pointing. CHRIS has the additional advantage of being relatively cheap and easy to manufacture since it has no moving parts. Its main applications is in environmental monitoring, forestry inventory and precision farming (Table 6.1).

The first version of the instrument flies on the PROBA (Project for On Board Autonomy) platform. It carries the instrument in a sun-synchronous elliptical polar orbit, at a mean altitude of about 600 km. All parts of the Earth's surface are accessible when PROBA's across track pointing ability is used.

From a 600 km orbit, CHRIS can image the Earth in a 14 km swath with a spatial resolution of 18 m (this is somewhat variable as the altitude varies around the orbit). Using PROBA's agile steering capabilities in along and across track directions enables observation of selectable targets well outside the nominal field of view of 1.3°. Images will generally be acquired in sets of 5, these being taken at along track angles of +/- 55 degrees, +/- 36 degrees, and as close to nadir as possible.

CHRIS operates over the visible/near infrared range from 400 nm to 1050 nm and can operate in 63 spectral bands at a spatial resolution of 36 m, or with 18 bands at full spatial resolution. Spectral sampling varies from 2-3 nm at the blue end of the spectrum, to about 12 nm at 1050 nm. Sampling is about 7 nm near the red edge (~690-740 nm). The instrument is very flexible and different sets of bands can be used for different applications (Table 6.2 and Figure 6.1).

¹ http://www.chris-proba.org.uk/mission/instrument_characteristics.html and <http://earth.esa.int/missions/thirdpartymission/proba.html>

Table 6.1: Specifications of the CHRIS-PROBA sensor

Spatial sampling interval	18 m on ground at nadir
Image area	14 km × 14 km (748 × 748 pixels)
Number of images	Nominal is 5 downloads at different view angles
Data per image (for a 14 × 14 km ²)	131 Mbits
Spectral range	410 nm to 1050 nm
Number of spectral bands	18 bands at a spatial resolution of 18 m, 63 at 36 m
Spectral resolution	1.3 nm @ 410 nm to 12 nm @ 1050 nm (i.e it varies across the spectrum)
Programmable operation	
Across track pixel size	18 m or 36 m
Along track pixel size	finest resolution is 18 m but can be made coarser by changing the integration time
Spectral	variable band width and location
Digitisation	12 bits
Signal-to-noise ratio	200 @ a target albedo of 0.2

The CHRIS instrument is programmable, so that a variety of band selections are possible. For this mission the number of different configurations is kept small. The principal configurations, based on a pre-launch wavelength calibration, are set out below in tables. Graphs are also provided, showing the locations of the bands compared to a typical spectrum of green vegetation, and to the spectrum of atmospheric absorption.

High Resolution, Full Swath (Land/Aerosol)

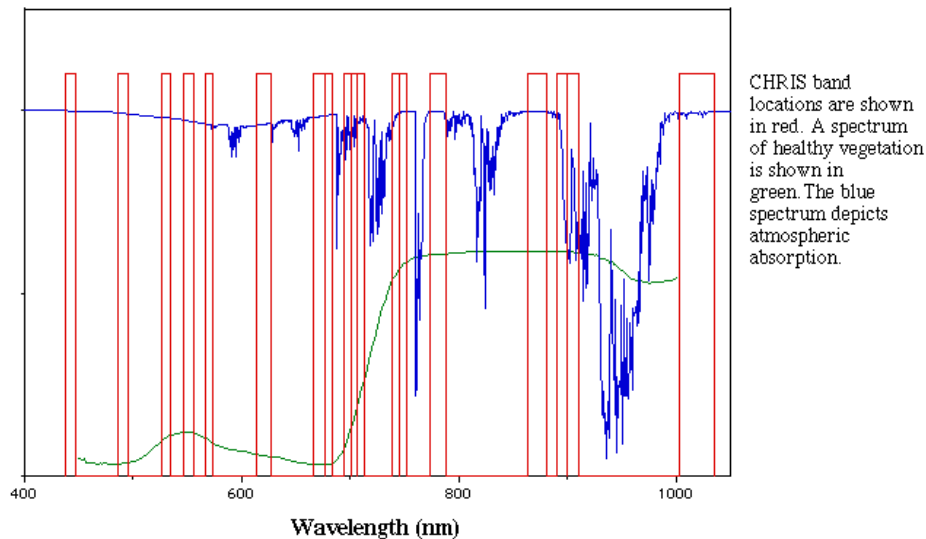


Figure 6.1: Band positions of the CHRIS-PROBA sensor for MODE 3 compared to a vegetation (green) and atmospheric (blue) spectrum.

Table 6.2: CHRIS PROBA bands For Full Swath, High Resolution Land/Aerosols (MODE 3).

Band	Detectors	From	To	lmid	Width
L1	41-45	438.0	446.8	442.4	8.8
L2	65-68	485.6	494.8	490.2	9.2
L3	81-83	525.6	534.2	529.9	8.6
L4	88-90	546.4	556.1	551.2	9.7
L5	94-95	566.3	573.4	569.8	7.7
L6	109-110	626.6	636.0	631.2	9.4
L7	115-116	655.8	666.3	661.0	10.5
L8	117-118	666.3	677.2	671.7	10.9
L9	122	694.3	700.1	697.2	5.9
L10	123	700.2	706.2	703.2	6.0
L11	124	706.2	712.4	709.3	6.2
L12	129	738.2	745.0	741.6	6.8
L13	130	745.0	751.9	748.4	6.9
L14	134-135	773.3	788.4	780.8	15.0
L15	145-146	863.1	881.3	872.1	18.3
L16	148	890.7	900.2	895.4	9.5
L17	149	900.2	909.8	905.0	9.7
L18	159-161	1002	1035	1019.0	32.9

CHRIS PROBA data were acquired for the area around the Millingerwaard on September 6, 2005 in MODE 3.

6.3 Assessment of data quality CHRIS PROBA data

When the CHRIS PROBA data were received no geometric or atmospheric correction procedures have been applied. The coverage of CHRIS PROBA data set is indicated in Figure 6.2.

Additional pre-processing steps and quality assessment are required before the images can be used to analyze vegetation distributions in the study area.



Figure 6.2: Coverage of CHRIS-PROBA data set for the area around Millingerwaard. As an example a colour composite of the nadir image is shown (no geometric and atmospheric correction).

7 Meteorological measurements

7.1 Haarweg station Wageningen

The weather station at the Haarweg in Wageningen is a special AgroMeteo-Station; the measurements include radiation and soil temperature. The coordinates of the location are 51° 58' NB; 5° 38' OL; and is about 7 metres above the sea level (see <http://www.met.wau.nl/>).

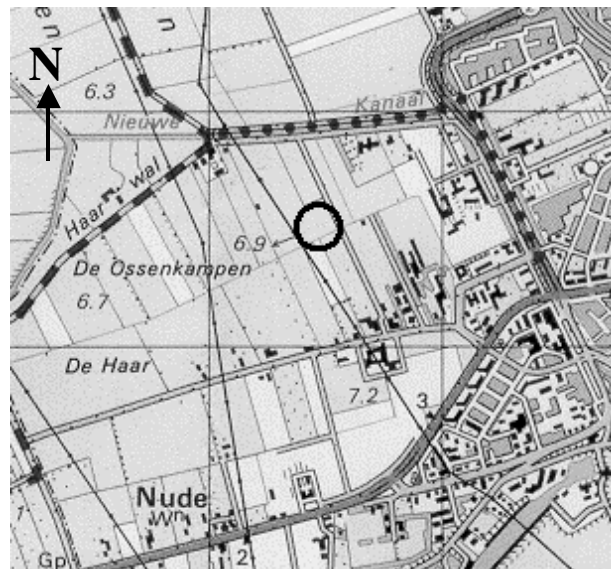


Figure 7.1: View of the location of the weather station (circle).

Table 7.1: Instruments at the weather station

Data	Instruments	Type
Relative humidity	Hair hygrometer	
Temperature and relative humidity	Thermo-Hygrometer	
	Ventilated Thermo-Hygrometer	
Air Pressure		
Wind speed at 4 levels	Cup anemometer (4x)	
Wind direction	Wind vane	
Short wave Radiation (global, reflected, net)	Pyranometers	Kipp en Zonen CM11
Long wave radiation	Pyrgeometer	
Amount of precipitation	Precipitation meter	Mierij Meteo
Precipitation duration	Precipitation meter	Thies
Sun duration	Sunshine Sensor	Kipp&Zonen CSD1
Soil temperature (bare soil and grass)	Thermocouple	PT 100
Sensible heat Flux	Large Aperture Scintillometer	Self construction

The following figures illustrate some of the meteorological measurements obtained at Wageningen on 19 June 2005. Net radiation, pressure and humidity are illustrated as hourly data for this day.

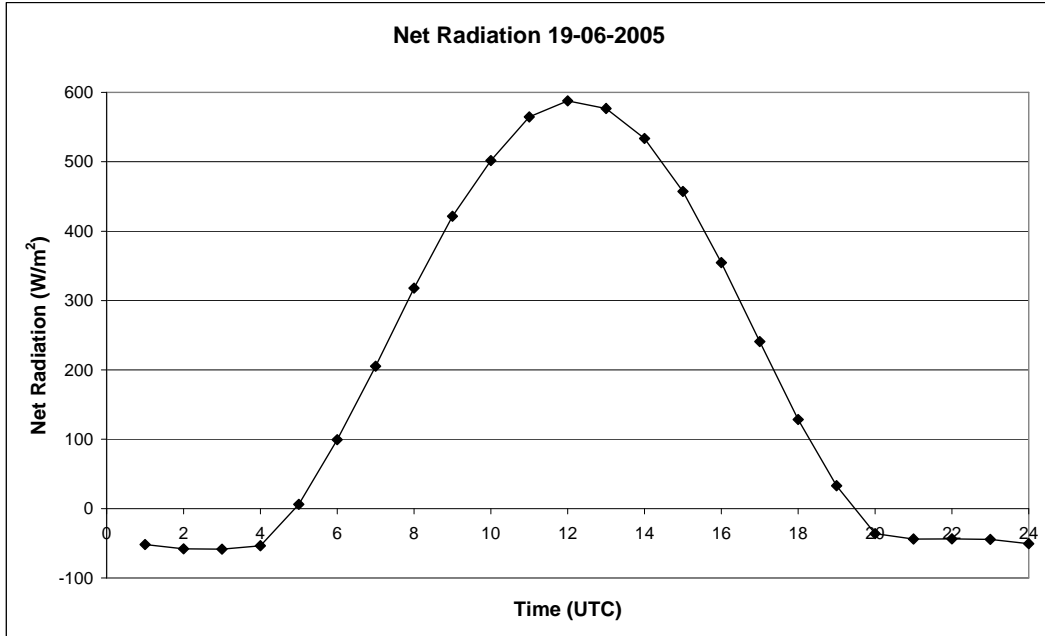


Figure 7.2: Average hourly net radiation at Wageningen on 19 June 2005

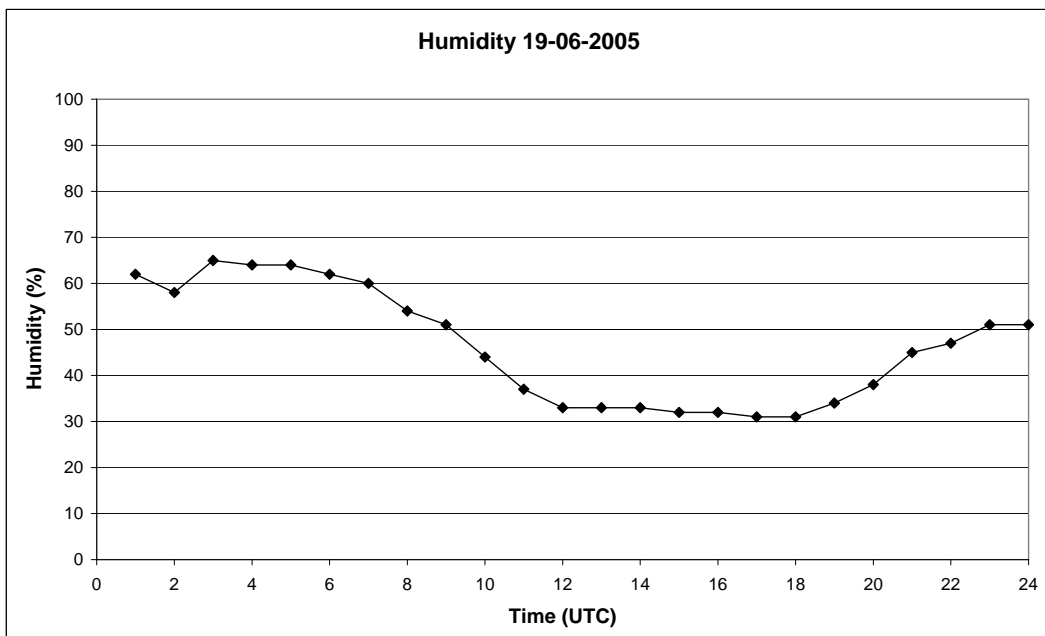


Figure 7.3: Average humidity at Wageningen on 19 June 2005

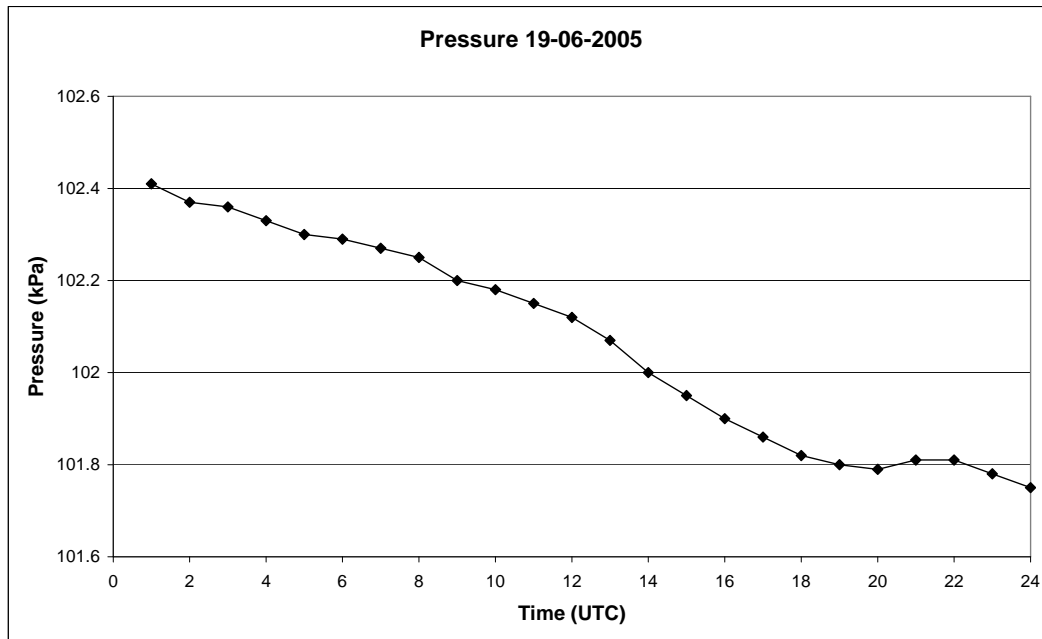


Figure 7.4: Average pressure at Wageningen on 19 June 2005

7.2 Observations Millingerwaard

On the day of the overflight of the AHS instruments two meteorological parameters were measured locally in the Millingerwaard. The aerosol optical depth (AOT) was measured using a Microtops II sunphotometer. More details on the instrument and the measurement methodology can be found in Kooistra et al. (2005).

For this campaign, measurements were performed on June 19, 2005 between 10:15 and 13:24 (GMT). Results for the 5 channels of the instrument are presented in figure 7.5. Visual inspection of the AOT values indicates that under these ‘clear sky’ conditions the variation in aerosol optical thickness is low.

A second instrument which was installed during the overflight was a pyranometer which measures the incoming solar radiation in kW/m^2 . The instrument uses small silicon-based photodetectors to measure the incoming radiation. The results for the Millingerwaard are presented in Figure 7.6 and show that June 19 was a very bright day with in fact no cloud influence.

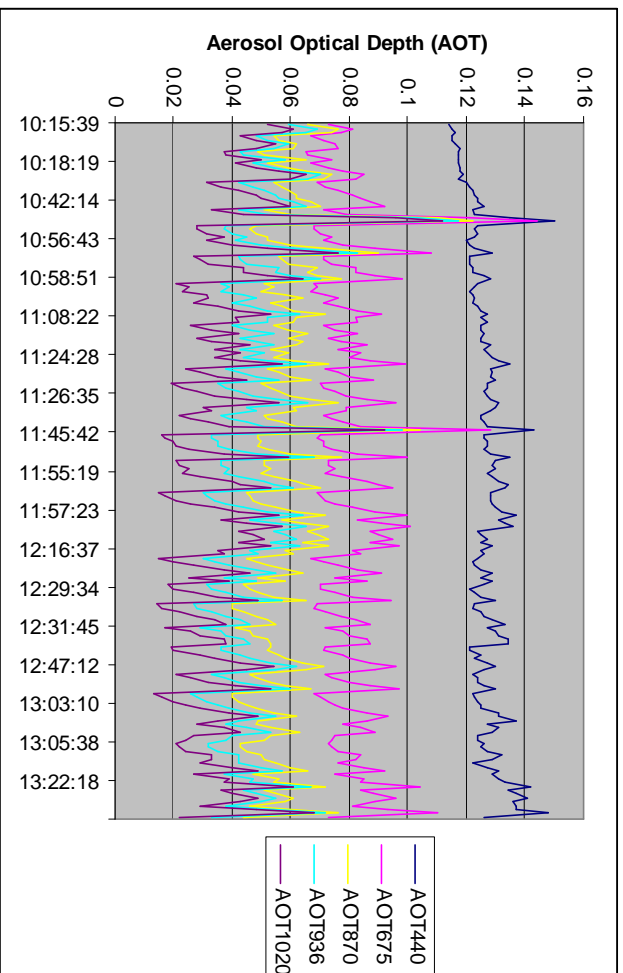


Figure 7.5: AOT values measured by the Microtops on 19 June 2005 in the Millingerward.

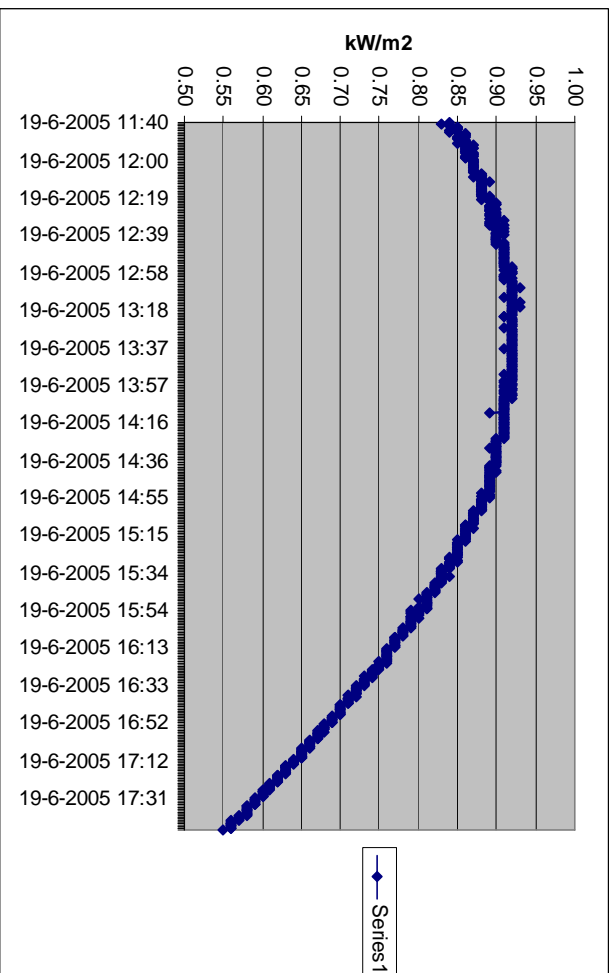


Figure 7.6: Incoming solar radiation measured by a pyranometer on 19 June 2005 in the Millingerward.

8 Land cover map Millingerwaard area

In order to be able to use the AHS images not just for the Millingerwaard floodplain, a land cover inventory was made for the area south-east of the Millingerwaard area in June 2005. Figure 7.1 depicts the land cover map produced.

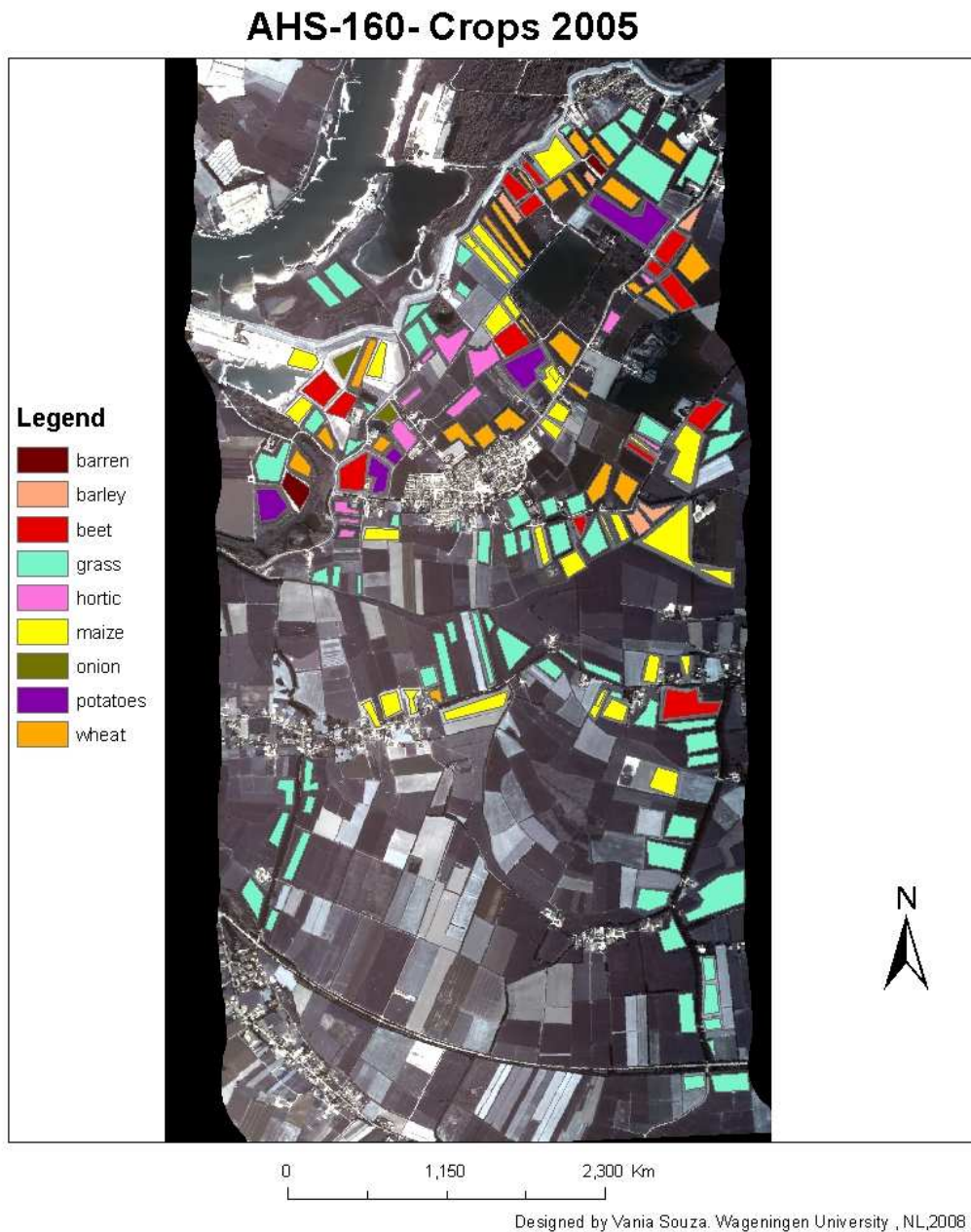


Figure 8.1: Land cover map for the Gelderse Poort area in 2005 (courtesy Vania Souza, Wageningen).

9 Soil moisture and temperature

During the day of the AHS acquisition measurements were made on the soil moisture and temperature status and vegetation temperature status for the 14 VALERI plots in the Millingerwaard. Measurements were made by colleagues from the Vrije Universiteit van Brussel. Details on the instrumentation and methodology can be found in Kooistra et al. (2005). Figure 9.1 and 9.2 give an overview of the results for the different VALERI plots.

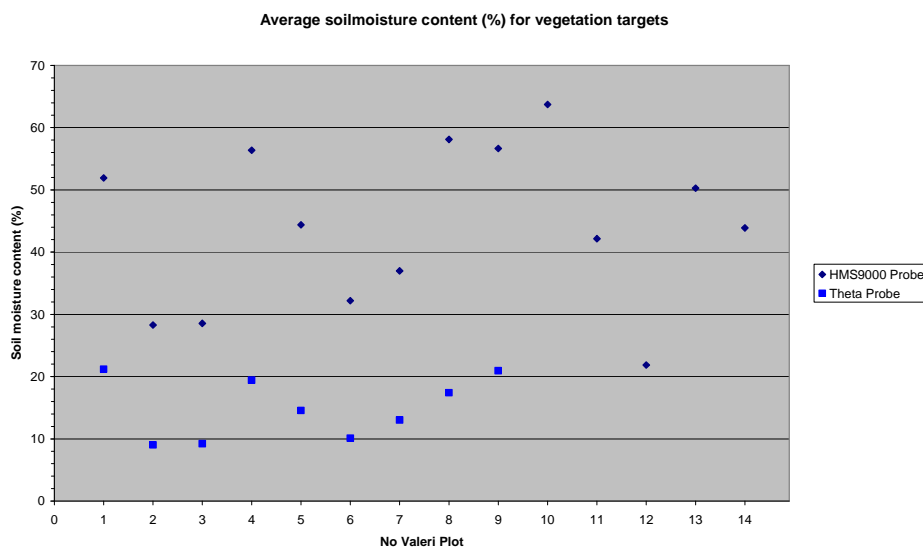


Figure 9.1: Measured soil moisture content for the locations of the vegetation plots in the Millingerwaard.

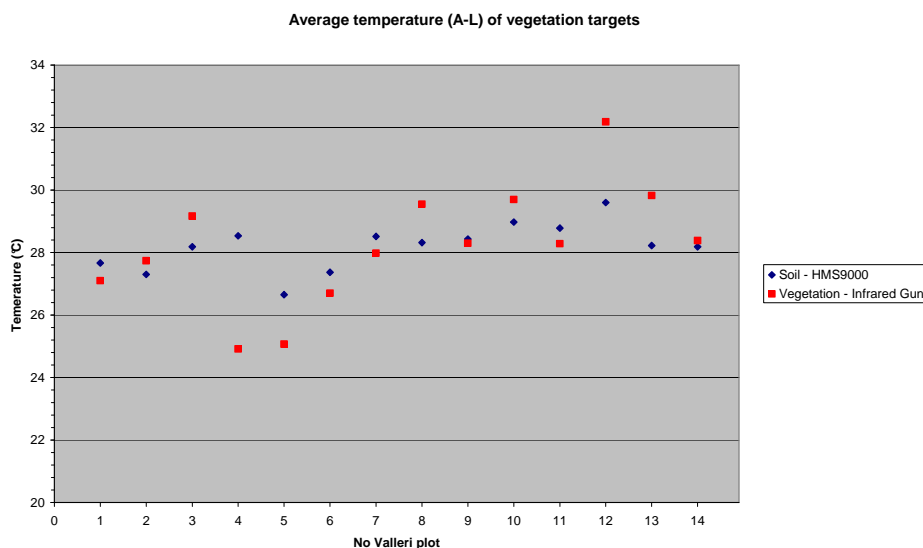


Figure 9.2: Measured soil and vegetation temperature for the locations of the vegetation plots in the Millingerwaard.

References

- Berk, A., G. P. Anderson, P. K. Acharya, J. H. Chetwynd, L. S. Bernstein, E. P. Shettle, M. W. Matthew & S. M. Adler-Golden, 1999. MODTRAN4 User's Manual, Air Force Research Laboratory, Hanscom, USA, 93 pp.
- Biesemans, J., S. Sterckx, E. Knaeps, K. Vrey, S. Adriaensen, J. Hooyberghs, K. Meuleman, P. Kempeneers, B. Deronde, J. Everaerts, D. Schläpfer, J. Nieke, 2007. Image processing workflows for airborne remote sensing. Proceedings 5th EARSel Workshop on Imaging Spectroscopy. Bruges, Belgium, April 23-25 2007
- Brand, A M, Aptroot, A, De Bakker, A J, Van Dobben, H F., 1988. Standaardlijst van de Nederlandse korstmossen. Wet Med KNNV 188:68 p.
- Braun-Blanquet, J., 1951. Pflanzensoziologie. Grundzüge der Vegetationskunde. Springer, Wien, 632 p.
- De Ronde, I., 2003. Vegetatieontwikkeling in de Millingerwaard aan de hand van herhaalde overzichtskaracteringen. MSc thesis, Centre for Geo-information and Department for Nature Conservation and Plant Ecology, Wageningen University, Wageningen.
- De Bruin, D., Hamhuis, D., Van Nieuwenhuijze, L., Overmars, W., Sijmons, D., and Vera, F., 1987. Ooievaar. De toekomst van het rivierengebied. Gelderse Milieufederatie, Arnhem (in Dutch).
- Fernandes, R., H. P. White, S. Leblanc, H. McNaim, J. M. Chen, and R. J. Hall, 2002. Examination of error propagation in relationships between leaf area index and spectral indices from Landsat TM and ETM. Draft.
- Gonsamo, A, 2006. Estimation Of Leaf Area Index Using Optical Field Instruments And Imaging Spectroscopy. Msc thesis, Centre for Geo-information, Wageningen University, Wageningen. Thesis Report GIRS-2006-09.
- Jonckheere, I., Fleck, S., Nackaert, K., Muys, B., Coppin, P., Weiss, M., and Baret, F., 2004. Review of Methods for in situ leaf area Index determination Part I. Theories, sensors and hemispherical Photography. Agricultural and forest metrology 121: 19-35.
- Kooistra, L., Sterckx, S., Liras Laita, E., Mengesha, T., Verbeiren, B., Batelaan, O., Van Dobben, H., Schaepman, M., Schaepman-Strub, G., and Stuijver, J., 2005. HyEco04: An airborne imaging spectroscopy campaign in the floodplain the Millingerwaard, the Netherlands. CGI-report 2005-07, Wageningen UR, Wageningen.

- Richter, R. & D. Schläpfer, 2002. Geo-atmospheric processing of airborne imaging spectrometry data. Part 2: atmospheric/topographic correction. *International Journal of Remote Sensing*, 23: 2631-2649.
- Richter, R., D. Schläpfer & A Müller, 2006. An automatic atmospheric correction algorithm for visible/NIR imagery. *International Journal of Remote Sensing*, 27: 2077-2085.
- Rodger A & M J Lynch, 2001. Determining atmospheric column water vapour in the 0.4-2.5 μm spectral region. In: *Proceedings of the AVIRIS Workshop 2001* (Pasadena, California, USA).
- Schaminee, J H J, Stortelder, A F H, Weeda, E J., 1996. *De vegetatie van Nederland 3: plantengemeenschappen van graslanden, zomen en droge heiden*. Opulus Press, Uppsala/Leiden, 356 p.
- Schaminee, J H J, Weeda, E J, Westhoff, V., 1995. *De vegetatie van Nederland 2: plantengemeenschappen van wateren, moerassen en natte heiden*. Opulus Press, Uppsala/Leiden, 360 p.
- Schaminee, J H J, Weeda, E J, Westhoff, V., 1998. *De vegetatie van Nederland 4: plantengemeenschappen van de kust en van binnenlandse pioniermilieus*. Opulus Press, Uppsala/Leiden, 346 p.
- Schläpfer, D. & R. Richter, 2002. Geo-atmospheric processing of airborne imaging spectrometry data. Part 1: parametric orthorectification. *International Journal of Remote Sensing* 23: 2609-2630.
- Touw, A, Rubers, W V., 1989. *De Nederlandse bladmossen - Flora en verspreidingsatlas van de Nederlandse Musci (Sphagnum uitgezonderd)*. KNNV Uitgeverij, Utrecht, 532 p.
- Van Der Meijden, R, Weeda, E J, Holverda, W J, Hovenkamp, P H., 1990. *Heukel's flora van Nederland*. Wolters-Noordhoff, Groningen, 662 p.
- Van Geloof, I. and De Ronde, I., 2002. *De vegetatie van de Millingerwaard na 10 jaar "natuurontwikkeling"*. MSc thesis, Centre for Geo-information and Department for Nature Conservation and Plant Ecology, Wageningen University, Wageningen.
- Weiss, M., Baret, F., Leroy, M., Begue, A., Hauteceur, O. and Santer, R., 1999. Hemispherical reflectance and albedo estimates from the accumulation of across track sun-synchronous satellite data. *Journal of Geophysical Research-Atmospheres*, 104(D18), 22221-22232.
- WWF, 1992. *Living Rivers*, WWF, Zeist.

Appendix 1 – AHS Quicklooks Millingerwaard 2005

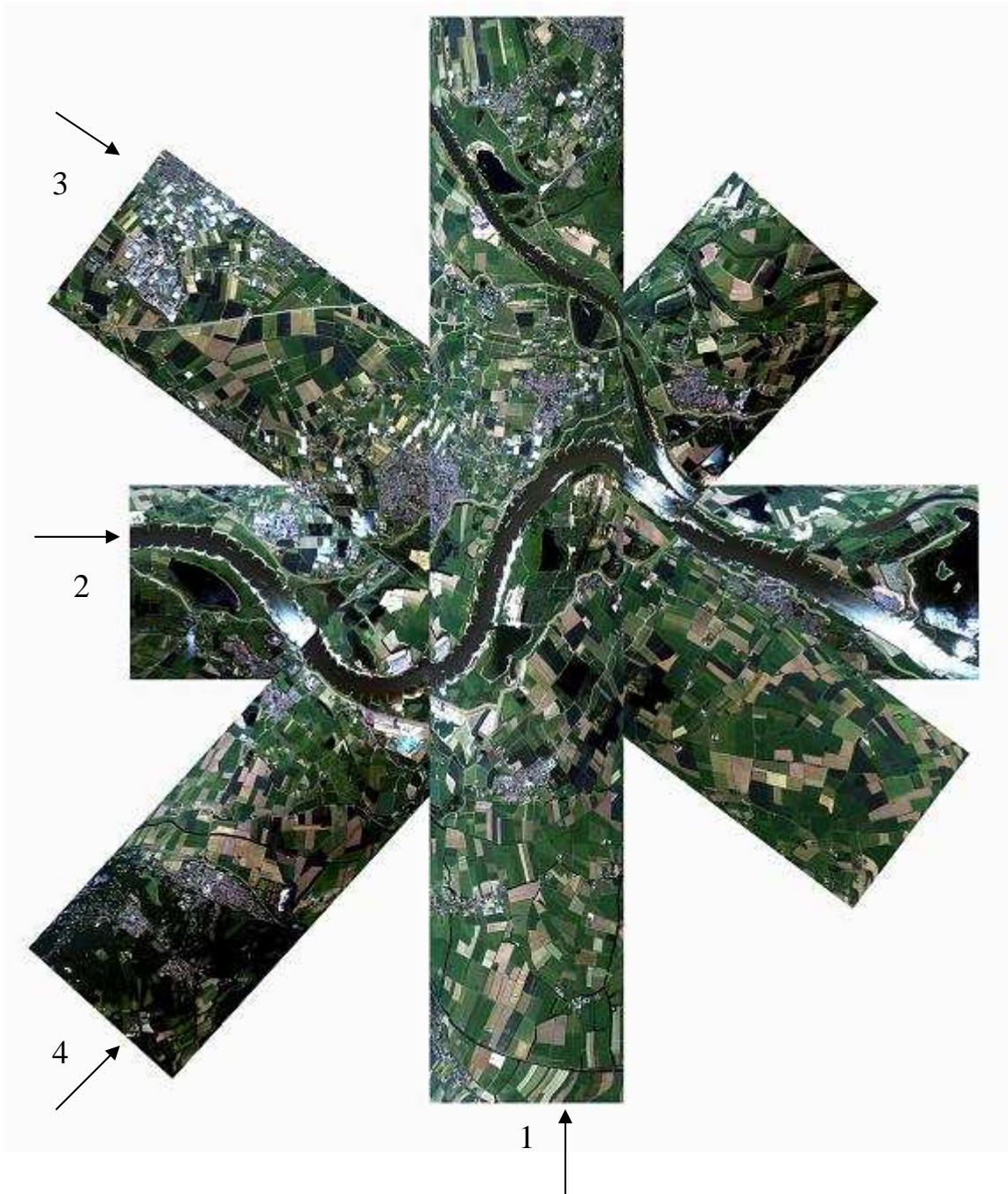




Table: Flight details 2005.

Acquisition Date	Flight line	Acquisition time (UTC)	Coordinates Flightlines (UTM/WGS84)				Altitude (feet/m, AGL)
			Start_Lat	Start_Lon	End_Lat	End_Lon	
19/06/2005	3	10:38	51.89209	5.95387	51.84386	6.03069	6000/1834
19/06/2005	1	10:46	51.83168	5.99209	51.90359	5.99306	6000/1834
19/06/2005	2	10:56	51.86781	5.95627	51.86744	6.02886	6000/1834
19/06/2005	4	11:04	51.84496	5.95460	51.88960	6.02983	6000/1834

This means:

Line 3 is flown NW – SE direction.

Line 1 is flown S – N direction.

Line 2 is flown W – E direction.

Line 4 is flown SW – NE direction.